UNIVERSITY OF GLASGOW

DEPARTMENT OF

AERONAUTICS & FLUID MECHANICS

A DIRECT VISCID–INVISCID INTERACTION SCHEME FOR THE PREDICTION OF 2–DIMENSIONAL AEROFOIL PERFORMANCE IN INCOMPRESSIBLE FLOW

by

F.N. COTON

R.A.McD. GALBRAITH

18 FEB 1987

G.U.AERO REPORT 8701

SUMMARY

This paper presents a method for assessing two-dimensional aerofoil performance characteristics including trailing edge and gross laminar separation. The model used is a direct viscid-inviscid interaction scheme based on a vortex panel method with boundary layer corrections and an inviscidly modelled wake. The integral boundary layer methods adopted behave well in the region of separation and thus, good comparisons with measured separation characteristics are obtained. Generally the predictions of lift and pitching moment may be considered to be within the experimental error, but where this is not the case, the applicability of the modelling technique is discussed.

List of Contents

	page
Nomenclature	2
1.0 Introduction	3
2.0 Description of the overall method	4
2.1 Inviscid Calculation	4
2.2 Boundary Layer Algorithm	6
2.2.1 Laminar Boundary Layer	7
2.2.2 Transition	7
2.2.3 Turbulent Boundary Layer	7
3.0 Results and Discussion	8
3.1 GA(W)-1	8
3.2 Gottigen 797	10
3.3 NACA 4412 and NACA 4415	10
3.4 GU25-5(11)8	11
4.0 Conclusions	13
Acknowledgements	14
References	15

NOMENCLATURE

s, y	Coordinates along and normal to surface
u, v	Velocities within the boundary layer in the s,y directions
u',v'	Boundary layer fluctuation velocities in the s,y directions
U_o	Freestream velocity
u_e	Velocity at edge of boundary layer
δ	Boundary layer thickness
δ^*	Boundary layer displacement thickness
θ	Boundary layer momentum thickness
ϵ	Boundary layer energy thickness
H	Momentum form parameter δ^*/θ
H_ϵ	Energy form parameter ϵ/θ
L	Ordinate of Le Foll's plane
X	Abscissa of Le Foll's plane
R	Reynolds number
ν	Kinematic viscosity
C_f	Skin friction coefficient
CD	Dissipation coefficient
C_L	Lift coefficient
C_{mq}	Pitching moment coefficient about quarter chord

Subscripts

c	Chord
s	Surface distance
θtr	Momentum thickness at transition

1.0 INTRODUCTION

For low cost aerofoil design applications, it is desirable to have a reliable predictive technique for assessing aerofoil performance. This is especially true in the region of "stall", where significant amounts of trailing edge separation may be present. The limited ability of current methods[1,2] is such that a final choice of section, for a given application, often requires extended wind tunnel tests. A major reason for this, is the uncertainty with which the location of separation is obtained. If, for a specified range of aerofoil types, the accuracy of predicting separation location could be improved to fall within experimental uncertainties, this would add confidence to the use of programs for the prediction of two-dimensional separated flow.

Separated flow over an aerofoil, as opposed to the fully-attached case, exhibits gross viscous effects which cannot be approximated by the inviscid calculation satisfying the classical Kutta condition. Such calculations[3] fail in the region of stall by over-predicting the lift coefficient as a consequence of neglecting separation. Existing analyses of these flows using the appropriate Navier-Stokes equations are costly, and currently yield results no better than simpler contemporary codes[4]. The simpler methods[2,5], it is commonly employ a viscid-inviscid interaction scheme. In such procedures the viscous boundary layer calculation yields sufficient information to effect appropriate displacement and local separation corrections, whilst the compatible inviscid calculation normally makes use of a standard panel method. The two computations are iteratively adjusted with respect to each other until some convergence criterion is satisfied. It is an interaction scheme of this type that is presented herein.

The present method forms the basis of, what is hoped will be, a useful design procedure for low Reynolds number aerofoils. The mathematical technique is of the direct type, where the predicted inviscid flow velocity distribution provides an input to the boundary layer calculation. Computed viscous displacement effects and the boundary layer separation point are then used to adjust the inviscid solution and so on. Modelling of the separated wake is achieved inviscidly in the manner of Dvorak and Maskew[6], using constant strength vortex panels, but as modified by Coton and Galbraith[7] for laminar separation cases. The capability therefore exists to cope with both laminar and turbulent separation at low speeds.

The technique, along with the specific constituent parts, is described and comparisons made with measured data for various aerofoils and Reynolds numbers. Specific problems associated with separation point calculation and boundary layer Reynolds number dependency are considered. Comment is made on how the input aerofoil coordinate data may influence the final result. Difficulties encountered in predicting laminar and turbulent separation effects are highlighted and the influence of the experimental environment on separation behaviour discussed. The overall effectiveness of the method and future development aims of the design procedure are discussed.

2.0 DESCRIPTION OF THE OVERALL METHOD

When separated aerofoil flows are modelled by means of a viscid-inviscid interaction method, the boundary layer equations are required to be 'matched' to an inviscid calculation[6]. In the direct mode, this is achieved by iteratively accounting for the displacement effect of the boundary layer, either by adjusting the aerofoil shape or by introducing an equivalent source distribution into the inviscid calculation; the sequence of this is as indicated in Fig. 1. It is the former technique that is employed herein. Some difficulty was encountered, however, in achieving calculation convergence due to the effect, on the inviscid calculation, of the rapid boundary layer growth at separation.

To overcome this, boundary layer displacement effects were only included when the calculation appeared to be nearing convergence. This resulted in a rapid approach to convergence followed by final small corrections, producing consistent results. Convergence was assumed to have been achieved when the separation point movement was less than 0.5% chord between successive iterations.

It was found that the rate of convergence was generally related to the extent of the separation present, with larger amounts of separated flow requiring a greater number of iterations. If, however, successively increasing angles of attack were calculated for the same aerofoil, then the carry over of the separation point from one incidence to the next, improved computational efficiency.

The viscid-inviscid interactive method adopted, divides the flow field into zones as depicted in Fig. 2. This figure illustrates the current state of the method, and it should be noted that it is capable of assessing the performance of aerofoils with either turbulent boundary layer separation towards the trailing edge or, at low Reynolds number, separations associated with the laminar boundary layer close to the leading edge.

Although a capability to model short separation bubbles is not included, the method does give an indication of long bubble formation by means of a previously reported technique[7]. The likely location for a short bubble formation is indicated by the existance of laminar separation prior to transition. Should such separation occur, however, the present procedure simply takes it to be the location of transition with the subsequent turbulent boundary layer calculation starting conditions taken from Horton's[8] mean reattachment velocity profile.

2.1 INVISCID CALCULATION

Use is made of the algorithm developed by Leishman et al[9]. to model the inviscid flowfield. This algorithm was developed from the panel method of Leishman and Galbraith[3] and exhibits the essential features of the method of Dvorak and Maskew[6]. In it, the aerofoil profile is replaced by an inscribed polygon of vortex panels over which the vorticity varies linearly, achieving piecewise continuity between adjoining panels. The

free shear layers used to model the aerofoil wake comprise of uniform strength vorticity panels. The distribution of all these vortex panels is illustrated in Fig.3.

The modelled wake region is assumed to be inviscid with negligible vorticity and is taken to have a constant total pressure equal to that at separation. It is further assumed that the free shear layers have no significant thickness and can be represented as streamlines across which there exists a velocity jump.

Each panel contains a control point at which the condition of flow tangency is applied. This is achieved by setting the scalar product of the induced velocity with the surface normal vector, to zero. This yields a set of linear simultaneous equations which, in conjunction with a specified Kutta condition (see Fig. 3), may be solved to yield the strength of the assumed vortex sheets, from which the required velocity distribution is obtained.

As part of the inviscid procedure, the wake shape is iteratively obtained from an initial shape estimate. The degree of correspondance which exists between the modelled and actual wake shape influences the acceptability of the final prediction[9]. Dvorak and Maskew[6] established that a practical initial wake shape may be obtained, by representing the location of the upper and lower free shear layers by parabolic curves with a common intersection point in the freestream. The shape of these curves is constrained by a Wake Factor; defined as the ratio of the wake length to wake height (Fig. 4). During the iterative process, the free vortex sheets of the wake are continually adjusted until they fall on a streamline. Three wake iterations are normally required, although up to six may be necessary for large areas of separated flow, due to the deterioration of the validity of the initial wake shape estimate.

For turbulent separation cases, the Wake Factor is taken as a constant for a given aerofoil shape and is related to the aerofoil thickness-chord ratio (Fig. 5a.). Unfortunately, for laminar separation, the shape of the wake is influenced by the distance the free shear layer covers prior to transition and, subsequently, by the rate of wake closure. It is, therefore, inappropriate to consider a constant wake factor. The present method utilises a previously developed correlation[7] between the momentum thickness Reynolds number at separation and the required increase in Wake Factor over that of the turbulent value. This relation, for laminar separation cases, is given in Fig. 5b. and was developed from a study of one aerofoil. Although it has been found to work well for the aerofoil considered, it can only be tentative at present.

For the fully attached flow case, the addition of the boundary layer displacement effect on the aerofoil contour produces a finite trailing edge, necessitating the use of an appropriate Kutta condition for solution. In the present "attached" method, separation is fixed at 0.995% chord, which produces a very small wake. The separated flow Kutta condition may thus be satisfied, retaining consistency in the programming and, as may be seen in Fig. 6., without any significant effect on the predicted pressure distribution.

2.2 BOUNDARY LAYER ALGORITHM

The laminar and turbulent boundary layer calculations are similar in that they are integral techniques based on the method of Le Foll[10]. This procedure requires the simultaneous solution of the momentum and energy integral equations over each calculative step. These equations (1 & 2) are cast in the form of Assassa and Papailiou[11] and are solved in the direct mode.

$$dq = C_1 dL - \frac{C_1 M}{1 + 2C_1 M} dX \qquad (1)$$

$$d\Phi = \frac{e^X dX}{(1 + 2C_1 M) CD\ e^{2C_1 L}} \qquad (2)$$

In the direct mode, the values of $d\Phi$ and dq, corresponding to the increment in stepsize Reynolds number and the velocity gradient respectivly, are necessary inputs. The boundary layer development is given by the change in Reynolds number based on a boundary layer characteristic length (dX) and the increment in the value of a profile form parameter (L). The following definitions apply :-

$$C_1 M = \frac{1}{H - 1}\left[1 - \frac{H_\epsilon\ C_f}{2\ CD} \right] \qquad (3)$$

$$X = \ln\left[\frac{\epsilon u_e}{\nu}\ e^{2C_1 L} \right] \qquad (4)$$

$$dL = \frac{1}{H - 1}\ \frac{dH_\epsilon}{H_\epsilon} \qquad (5)$$

$$\Phi = \int_0^s \frac{u_e}{\nu}\, ds \qquad (6)$$

$$q = \ln \frac{u_e}{U_o} \qquad (7)$$

The functions L and X are well behaved at separation which, for both the laminar and turbulent calculations, is indicated by vanishing skin friction.

Specification of the above functions is facilitated by way of suitable velocity profile families.

2.2.1 Laminar Boundary Layer

During the initial development of the overall procedure, the laminar boundary layer calculation was by the method of Head[12]. This procedure, was specifically developed for use with a slide-rule and, whilst, apparently very accurate, was, when configured for computer use, slow and required a large number of steps per calculation. It was evident that the method's good performance was related to the accurate doubly-infinite velocity profile family on which it was based. The present method utilises relations derived from this family to provide skin friction and dissipation coefficient values and to effect closure of the above system of equations. The method, while apparently retaining the accuracy of Head's technique, is computationally more efficient.

2.2.2 Transition

There are at present three transition options available within the code. Transition can be fixed, calculated or, as stated previously, taken to occur at the point of laminar separation. If transition is fixed, then the required input to the program is the chordwise location. The location of natural transition is obtained using the correlation of Cebeci et al[13].

$$R_{\theta tr} = 1.174 \left[1 + \frac{22400}{R_s} \right] R_s^{\,0.46} \qquad (8)$$

Whilst this correlation is suitable for high Reynolds numbers, it may require modification to account for low Reynolds numbers.

The third transition option is as described previously, but with the additional capability to alter the turbulent boundary layer starting velocity profile shape.

2.2.3 Turbulent Boundary Layer

For the turbulent boundary layer, Coles[14] velocity profile family (in the more generalised form of Khun and Neilsen[15]) is used, together with the Nash π-G relationship[16], to provide the velocity profiles and skin

friction at each station in the calculation and to effect closure. The value of the dissipation coefficient is obtained via a semi-empirical relationship[11]. The influence of the second order terms, i.e. normal stresses, on the turbulent boundary layer calculation is included by setting the value of the constant C_1 to 0.85, i.e.

$$C_1 = \frac{H - 1}{H^* - 1} = 0.85 \qquad (9)$$

Where

$$H^* = \frac{\delta^*}{\theta^*} \qquad (10)$$

And

$$\theta^* = \theta - \int_0^{\delta} \frac{\overline{u'^2} + \overline{v'^2}}{u_e} \, dy \qquad (11)$$

The second order terms can be neglected by assigning the value of unity to C_1 in the laminar boundary layer calculation.

3.0 RESULTS AND DISCUSSION

To assess the predictive capability of the developed method, a number of comparisons with wind tunnel data were made. These data were obtained for a variety of test facilities and cover the Reynolds number range $5x10^4$-$6x10^6$. The input coordinate data to the program was as published[17,18,19], except for the two NACA sections which were computer generated from standard functions[20]. For turbulent separation cases, comparison was made between theory and experiment for four aerofoils of varying section. The relative dearth of data at very low Reynolds number has, at present, limited the study of laminar separation to the GU25-5(11)8 aerofoil[21]. In the cases where experimentally obtained pressure data were available, comparison has been made with the computed distributions.

3.1 GA(W)-1

This section was originally developed for general aviation purposes but has also been extensively used in wind energy generation and more recently on microlight aircraft. The aerofoil is a 17% thick section with the maximum thickness lying at approximately 40% chord.

The experimental data for the GA(W)-1 aerofoil which were obtained in the NASA Low Turbulence Pressure Tunnel[17] (LTPT) has been used on a number of occasions[6,22] for assessing predictive accuracy. This aerofoil exhibits

a classic trailing edge type stall with the separation point moving relatively slowly from the trailing edge to the leading edge on the upper surface. This type of stall is ideal for analysis by most predictive schemes, since the unusual viscous effects, often present when rapid separation point movement occurs, do not require to be accounted for.

Negative angles of attack were calculated by inverting the aerofoil and then calculating for positive incidences.

In Fig. 7. comparison is made, between the lift and pitching moment coefficients, for three Reynolds numbers. At $R_c=2x10^6$, the general trend of the lift curve is predicted, albeit there are some deviations, notably at 8 and 12 degrees. The anomaly at 8 degrees arises from the position of upper surface separation being almost coincident with the trailing edge. The assosciated rapid thickening of the boundary layer produces an abnormal discontinuity in the profile shape which, in turn, results in an uncharacteristic orientation of the trailing edge wake. To alleviate this problem, the growth of the boundary layer was restricted if separation was predicted after 95% chord. Even with this restriction, however, some deviation still existed, as is apparent from the figure. A similar effect is evident at the highest Reynolds number for an incidence of 10 degrees.

To account for viscous effects between iterations, the aerofoil contour was adjusted via a suitable displacement of the panel corner points. This made the modelling of rapid boundary layer growth, within a panel, a most difficult procedure. It was particularly relevent to the panel containing the separation point, and manifested itself via the calculated value of C_L at 12 degrees incidence (Rc=2000000) where it may be observed that a marked over-prediction was obtained.

For all three Reynolds numbers considered, the pitching moment coefficients for negative incidences, were under-predicted. Although there was no apparent reason for this discrepancy, the calculated lift was slightly higher than that measured. This indicated that too much lower surface separation was predicted resulting in a reduced pitching moment. When relatively large areas of separated flow exist over an aerofoil, the constant pressure region aft of the separation point can have a significant influence on the value of pitching moment coefficient. This would appear to be the case in Fig.7. for $R_c=6x10^6$,where the calculated value in the region of stall was higher than the measurements.

The predicted value of maximum lift was good for the lowest Reynolds number considered but was slightly poorer for the other two cases. The least satisfactory prediction was obtained at $R_c=4x10^6$ where, after stall, a progressive under-prediction of the value of lift coefficient occured. In this case, the difference between the two maximum lift values was about 3% and the stall angle was in error by 0.5 degrees.

Figure 8 presents selected comparisons of calculated and empirical pressure distributions at the highest Reynolds number. Generally, the values of peak suction are in agreement except at 12.04 degrees where the separation point was near the trailing edge and the pressure distribution was therefore subject to the above mentioned trailing edge effects. The pressure distributions for 16.04 and 20.05 degrees show some discrepancy

between measured and calculated separation points. The predicted movement of the separation point, through the angle of attack range, was found to be influenced by the polygonal panel distribution and the relative position of separation within a panel. In each of the two cases, however, the apparent separation point on the measured distribution was within one panel length of the predicted position.

The current modelling of the wake by a constant Wake Factor would appear to be reasonably satisfactory for turbulent separation cases, since, for the four distributions presented, there is good agreement between the predicted and measured profiles.

3.2 GOTTIGEN 797

An example of the effect of the panel distribution on the movement of the separation position can be seen in Fig. 9. Here the predicted separation characteristics, for the Gottigen 797 aerofoil, are compared with those obtained experimentally[18]. The measured separation front exhibited a monotonic variation whilst the predicted values progressed in a steplike manner. There was, however, no associated stepping effect on the lift curve (Fig. 9.), although, some degree of discontinuity was apparent and was undoubtedly linked to the behaviour of the boundary layer on the separation panel. At all angles of attack, the prediction of separation was within 5% chord of the experimental location and the general trend of the two separation characteristics was similar.

The difference in maximum lift values was about 6%, and this occurred at the point of greatest disagreement in the separation characteristics. The overall agreement may have been improved by a more appropriate panel distribution but, since it was intended to establish the performance of the predictive scheme, using the test-model coordinates as panel corner points, no such modification was attempted.

3.3 NACA 4412 and NACA 4415

These two aerofoil sections are typical of many in general use and, as such, provide good test cases for predictive codes. The wind tunnel tests, which provided the empirical data, were conducted in the NASA Low-turbulence tunnel facility[23] and at Reynolds numbers from 1×10^6 to 3×10^6.

In figure 10 lift coefficient characteristics are presented at three Reynolds numbers for the NACA 4412 section. In all three cases, the empirical and predicted lift curve slopes are in good agreement. The initiation of separation, however, is accompanied by a discontinuity in the predicted curve. This condition only exists for approximately one degree in the incidence range. The prediction of maximum lift is within 3.5% of the experimentally obtained value for all three Reynolds numbers although, for $R_c=2\times10^6$ and $R_c=3\times10^6$, stall is predicted one degree earlier than experiment would indicate. Such a difference in stall angle may be

due to a number of effects, such as wind tunnel blockage or differences between the model geometry and the generated aerofoil coordinates.

Of all the test cases considered, the NACA 4415 aerofoil has proved the most difficult to predict, albeit the corresponding lift curve slopes (Fig. 11.) show good agreement. At the lowest Reynolds number, however, there was a significant over-prediction of both maximum lift and the stall angle. This particular case indicated the presence of a laminar separation bubble and so the current inability to account for these and their subsequent effect on the turbulent boundary layer growth, influenced the predictive accuracy.

One effect of a separation bubble can be to cause earlier turbulent boundary layer separation and thus enhance the stall. An increased Reynolds number would tend to reduce the influence of a bubble on the maximum lift. This appeared to be the case here, since the aggreement improved at the two higher Reynolds numbers. Although there were some discontinuities in the lift curves around the stall, the maximum lift was within 4% of the empirical value in both cases.

3.4 GU25-5(11)8

The GU25-5(11)8 aerofoil was developed as one of a family of sections specifically for man-powered flight and to date remains the only one to have been wind tunnel tested[19]. The aerofoil has been used for a number of applications, most notably as the canard wing of several microlight aircraft. Recently, some very low Reynolds number wind tunnel tests were conducted[21] to assess its low Reynolds number performance. It was found, that the aerofoil exhibited gross laminar separation, at all positive angles of attack, below $R_c=1x10^5$, and that the loss in lift associated with this condition was substantial. Comparisons between the lift characteristics above and below $R_c=1x10^5$, along with predicted values for the lower Reynolds number case, are presented in Figure 12.

At low incidence, the prdicted values of lift coefficient were higher than the measurement which was probably a consequence of an inability account for the observed lower surface separation. Throughout the angle of attack range, there were several discontinuities in the calculated and empirical lift curves. The former was due to the susceptibility of the pressure distribution to the separation point when such a large region of separated flow exists, and the latter to the practical difficulties in obtaining data at such low Reynolds numbers. It is suggested, that the variance in the calculated values, however, lies within the experimental tolerance.

In Figure 13 the calculated and empirical pressure coefficient distributions at 12.6 degrees are presented for three Reynolds numbers. At $R_c=1x10^5$ there is poor agreement in the location of separation. This arose from the constraint of using given wind tunnel model coordinates, which limited the input polygon to less than fifty panels, thus reducing the acheivable accuracy of the inviscid calculation and the subsequent separation point determination.

A limitation of the present approach is highlighted in the pressure coefficient distribution for $R_c=1.5x10^5$. Here the measured pressure coefficients in the separated region increased towards the trailing edge. This is typical of a wake which, after transition, closes rapidly towards the trailing edge. The pressure distribution produced by such a wake resembles that of a long separation bubble, albeit no re-attachment occurs on the aerofoil. The evident recovery is enhanced with increasing Reynolds number, until a long separation bubble is formed. Such a condition cannot be effectively modelled by a constant pressure wake, but, in the present method, a warning of when this condition is likely to exist is given by the long bubble reattachment criterion[7].

4.0 CONCLUSIONS

(1) A direct viscid-inviscid interaction scheme for modelling both laminar and turbulent separation on a 2-D aerofoil section has been developed.

(2) For the test cases presented, the agreement between prediction and measured data has been good; even at stall.

(3) The effect of polygonal panel distribution and the behaviour of the boundary layer on the separation panel require more investigation.

(4) Inclusion of a separation bubble model would be desirable for predicting low Reynolds behaviour.

(5) For some laminar separation cases, the constant pressure wake model may be inappropriate. This probably occurs when the upper free shear layer is about to reattach in the region of the trailing edge.

ACKNOWLEDGEMENTS

The authors wish to acknowledge the encouragement and support of Professor B.E. Richards of Glasgow University and Mr. P. Swan of British Aerospace plc.

The work was carried out in collaboration with British Aerospace plc via SERC CASE Award No. EB.048

REFERENCES

1. Liebeck, R.H., 'Design of Subsonic Airfoils for High Lift', Journal of Aircraft, Vol 15,

2. McMasters, J.H., Henderson, M.L., 'Low-Speed Single Element Airfoil Synthesis', Technical Soaring, Vol. 6, No. 2, pp.1-21, (1979)

3. Leishman, J.G., Galbraith, R.A.McD., 'An Algorithm for the Calculation of the Potential Flow about an Arbitrary Two-Dimensional Aerofoil', Glasgow University Aero. Report No. 8102 (1981)

4. Mueller, T.J., 'Low Reynolds Number Vehicles', AGARDograph No. 288, (February 1985).

5. Williams, B.R., 'The Calculation of Flow about Aerofoils at Low Reynolds Number with Application to Remotely Piloted Vehicles', International Conference on Aerodynamics at Low Reynolds Numbers (10^4<Re<10^6), London, (1986)

6. Maskew, B., Dvorak, F.A., 'The Prediction of C_{Lmax} Using a Separated Flow Model', Journal of the American Helicopter Society, (1978)

7. Coton, F.N., Galbraith, R.A.McD., 'A Simple Method For The Prediction of Separation Bubble Formation on Aerofoils at Low Reynolds Number', International Conference on Aerodynamics at Low Reynolds Numbers (10^4<Re<10^6), London, (1986)

8. Horton, H.P., 'A Semi-Empirical Theory for the Growth and Bursting of Laminar Separation Bubbles', ARC. C.P. No. 1073, (1969)

9. Leishman J.G., Galbraith, R.A.McD., Hanna, J., 'Modelling of Trailing Edge Separation on Arbitrary Two-Dimensional Aerofoils in Incompressible Flow Using an Inviscid Flow Algorithm', Glasgow University Aero. Report No. 8202 (1982)

10. Le Foll, J., 'A Theory of Representation of the Properties of Boundary Layers on a Plane', Proc. Seminar on Advanced Problems in Turbomachinery, V.K.I., (1965)

11. Assassa, G.M., Papailiou, K.D., 'An Integral Method for Calculating Turbulent Boundary Layer with Separation', Transactions of the ASME, Vol. 100, pp.110-116 (1979)

12. Head, M.R., 'An Approximate Method for Calculating the Laminar Boundary Layer in Two-Dimensional Incompressible Flow', ARC. R & M No. 3123, (1959)

13. Cebeci, T., Smith, A.M.O., 'Analysis of Turbulent Boundary Layers', Applied Mathematics and Mechanics, Vol. 15, Academic Press, London, (1974)

14. Coles, D., 'The Law of the Wake in the Turbulent Boundary Layer', C.I.T. Report, (1955)

15. Khun, G.D., Neilsen, J.N., 'Prediction of Turbulent Separated Boundary Layers', AIAA Journal, Vol. 12, No. 7, pp.881-882, (1974)

16. Nash, J.F., 'Turbulent Boundary Layer Behaviour and the Auxiliary Equation', AGARDograph 97, part 1, pp.245-279, (1965)

17. McGhee, R.J., Beasley, W.D., 'Low-Speed Aerodynamic Characteristics of a 17-Percent-Thick Airfoil Section Designed for General Aviation Applications', NASA TN D-7428, (1973)

18. Render, P.M., 'The Experimental and Theoretical Aerodynamic Characteristics of Aerofoil Sections Suitable for Remotely Piloted Vehicles', CoA Report No. 8419, (1984)

19. Kelling, F.H., 'Experimental Investigation of a High-Lift Low-Drag Aerofoil', Glasgow University Report No. 6802, (1968)

20. Ladson, C.L., Brooks Jr., C.W., 'Development of a Computer Program to Obtain Ordinates for NACA 4-Digit, 4-Digit Modified, 5-Digit, and 16-Series Airfoils', NASA TM X-3284, (1975)

21. Galbraith, R.A.McD., 'The Aerodynamic Charateristics of a GU25-5(11)8 Aerofoil for Low Reynolds Numbers', Glasgow University Report No. 8410 (1984)

22. Blascovich, J.D., 'A Comparison of Separated Flow Airfoil Analysis Methods', Journal of Aircraft, Vol. 22, No. 3, (1984)

23. Miley, S.J., 'A Catalog of Low Reynolds Number Airfoil Data for Wind Turbine Applications', Aerospace Engineering Dept., Texas A & M University, (1982)

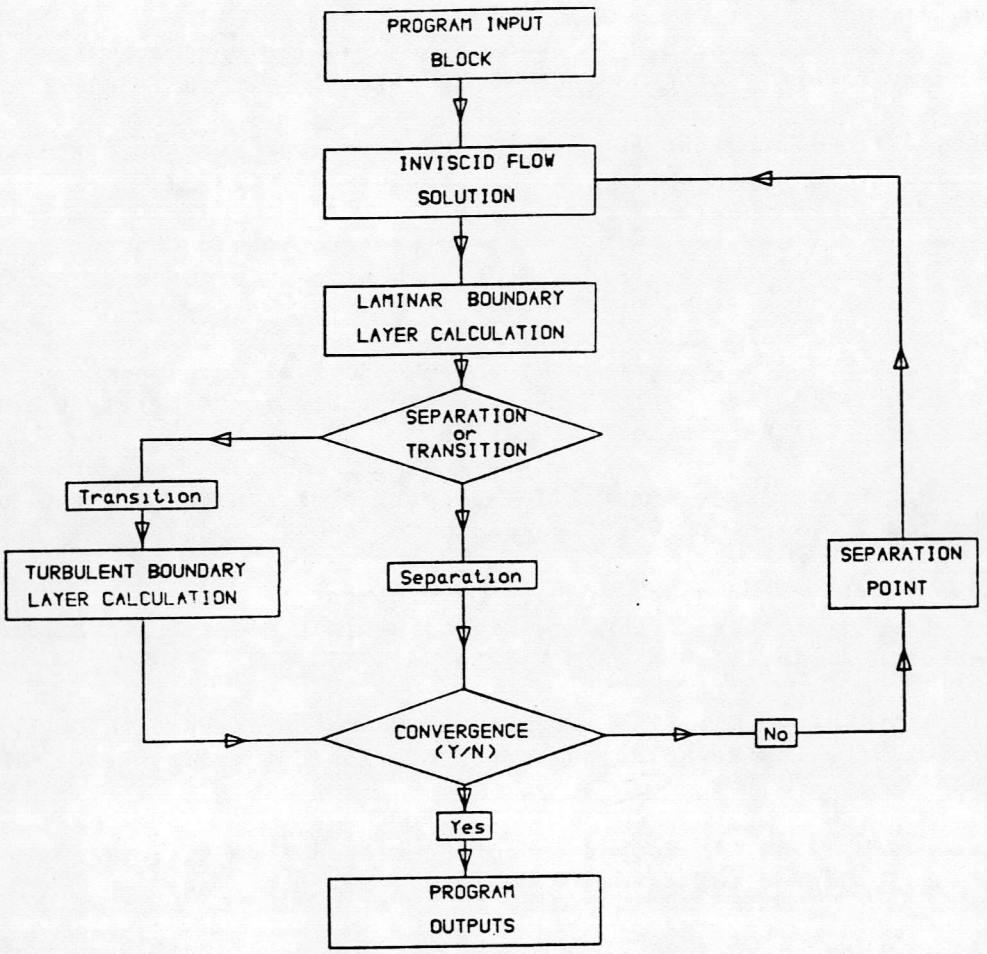

Fig. 1. Program Flow Chart

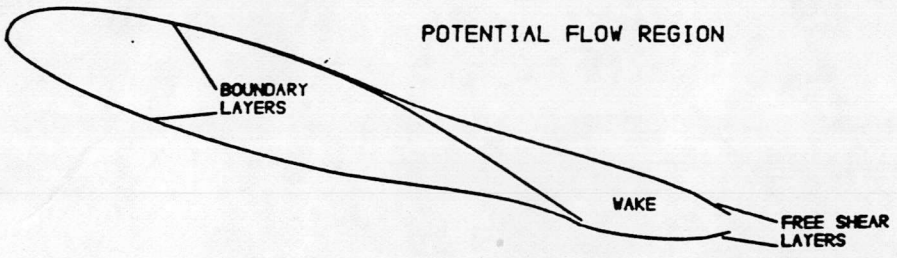

Fig. 2. Regions of the Mathematical Model

• Control points

× Wake iteration control points

Specified Kutta Condition : $\gamma_{sep} + \gamma_{N+1} = 0$

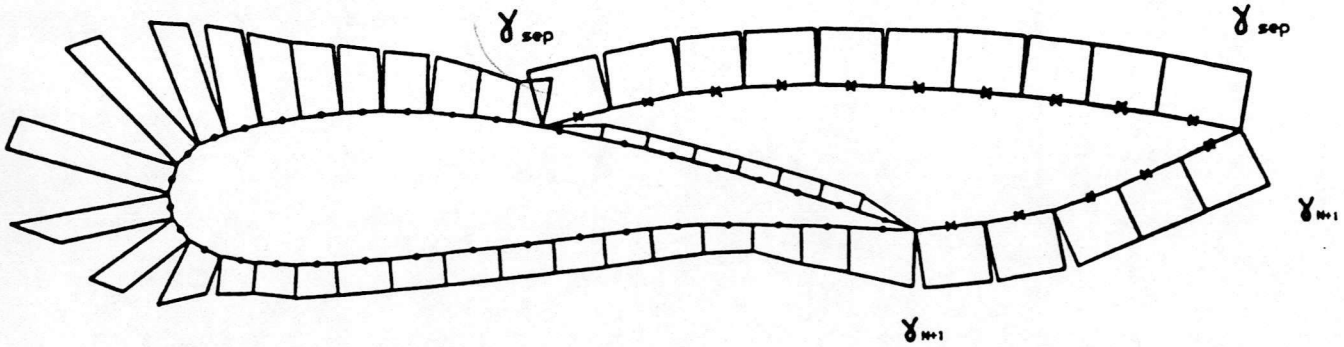

Fig. 3. Polygonal Panel Vorticity Distribution

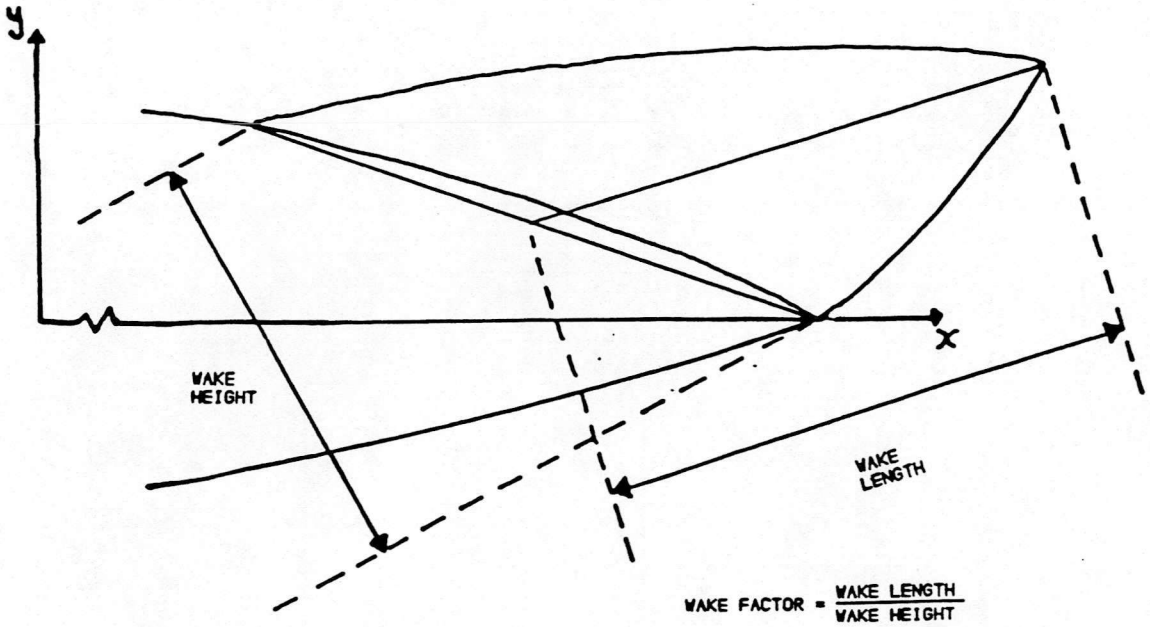

Fig. 4. Calculation of Wake Factor

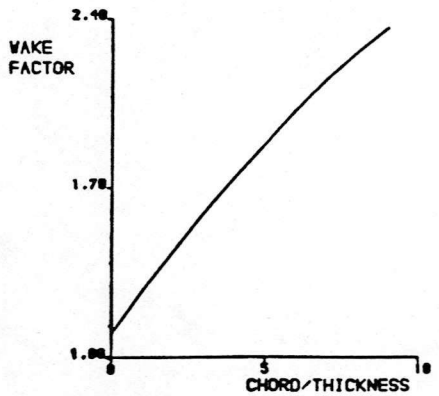

Fig. 5a. Wake Factor Correlation

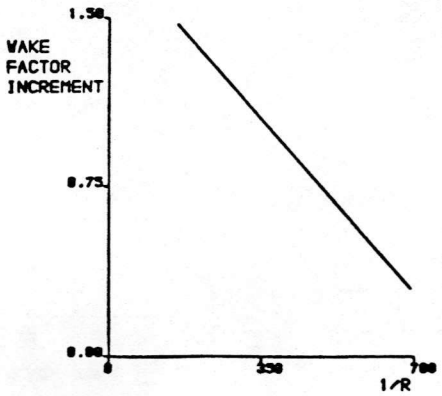

Fig. 5b. Increment Correlation

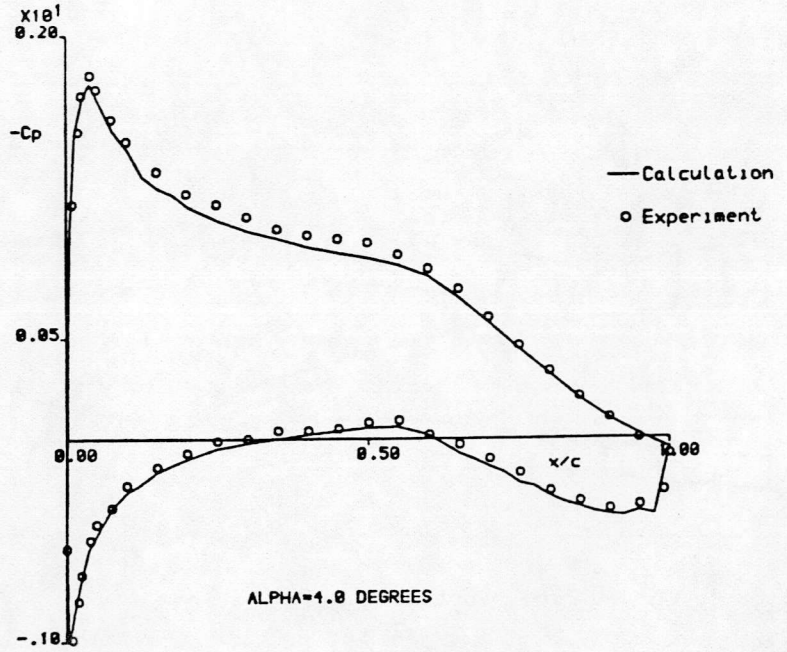

Fig. 6. Comparison of calculated and experimental Cp distribution for the GA(W)-1 aerofoil at 4.0 Degrees.

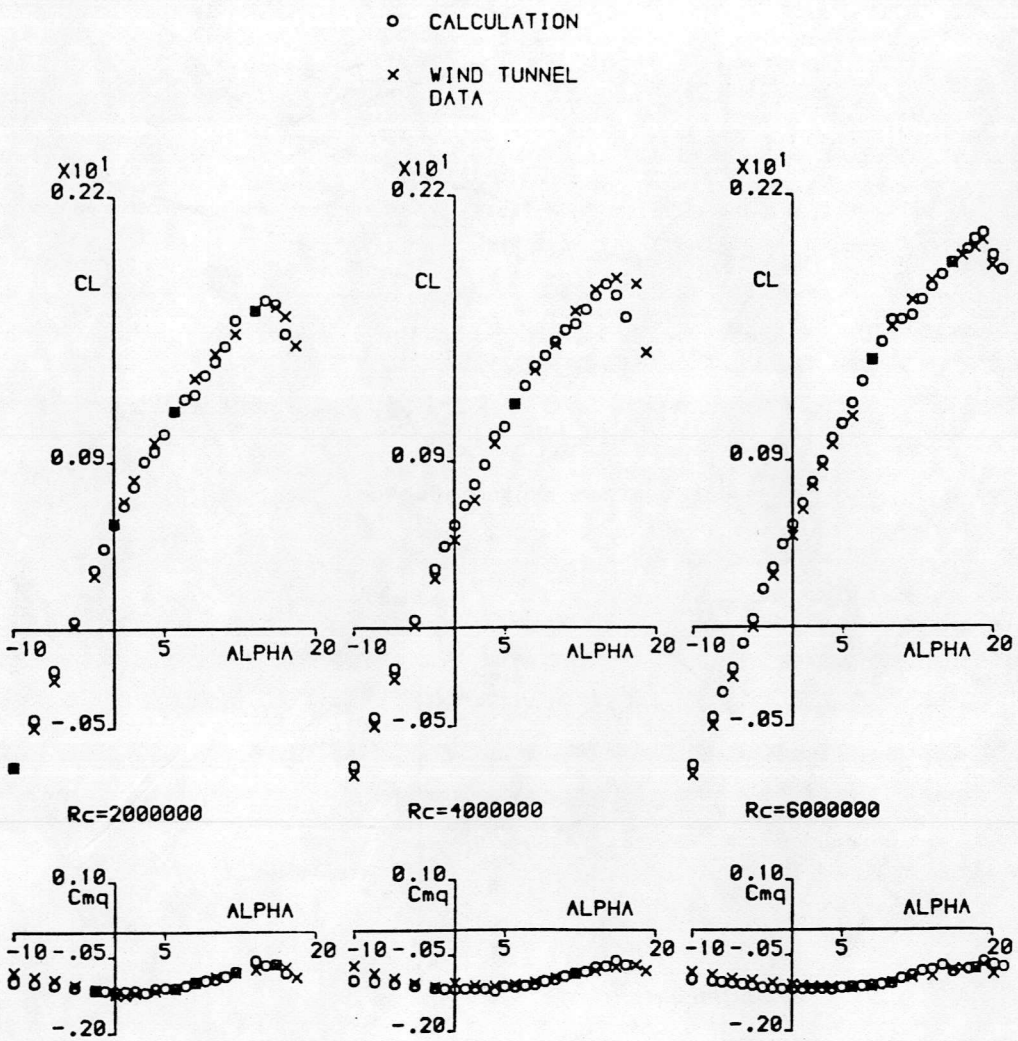

Fig. 7. Comparison of calculation with wind tunnel data For the GA(W)-1 at three Reynolds numbers.

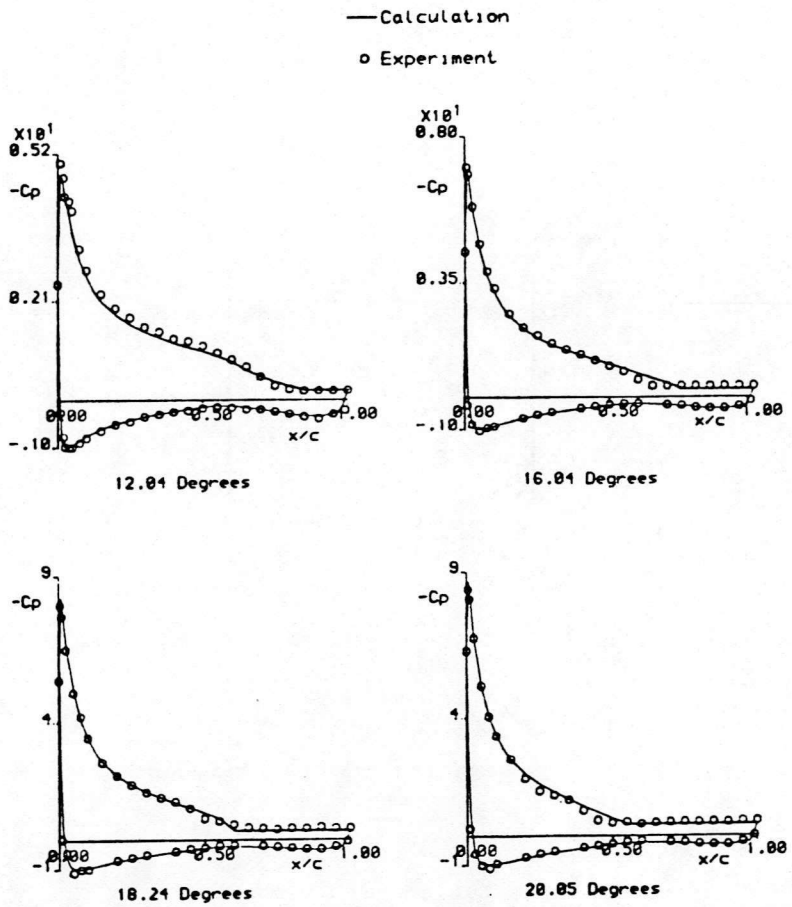

Fig. 8. Comparison of calculated and experimental Cp distributions for the GA(W)-1 aerofoil at four angles of attack, Rc=6000000.

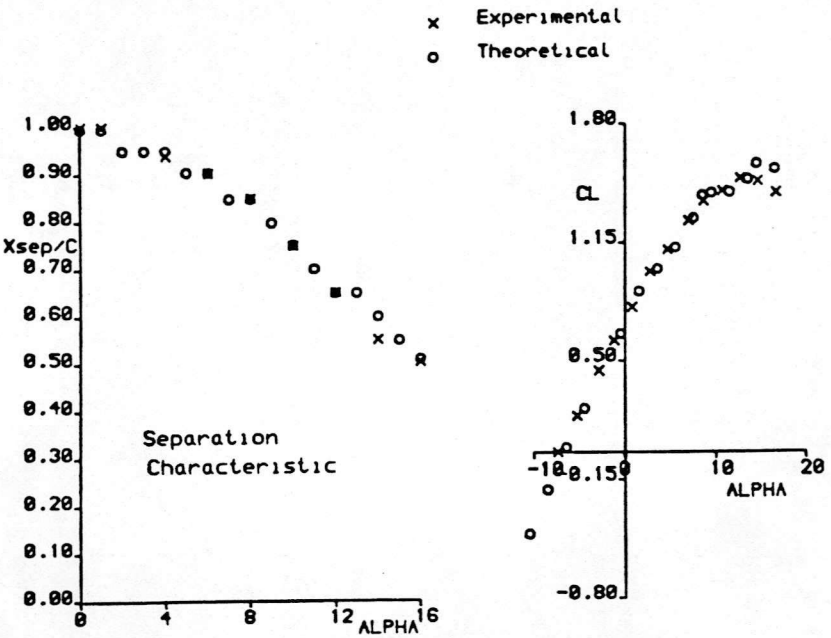

Fig. 9. Gottigen 797 Aerofoil at Rc=1000000

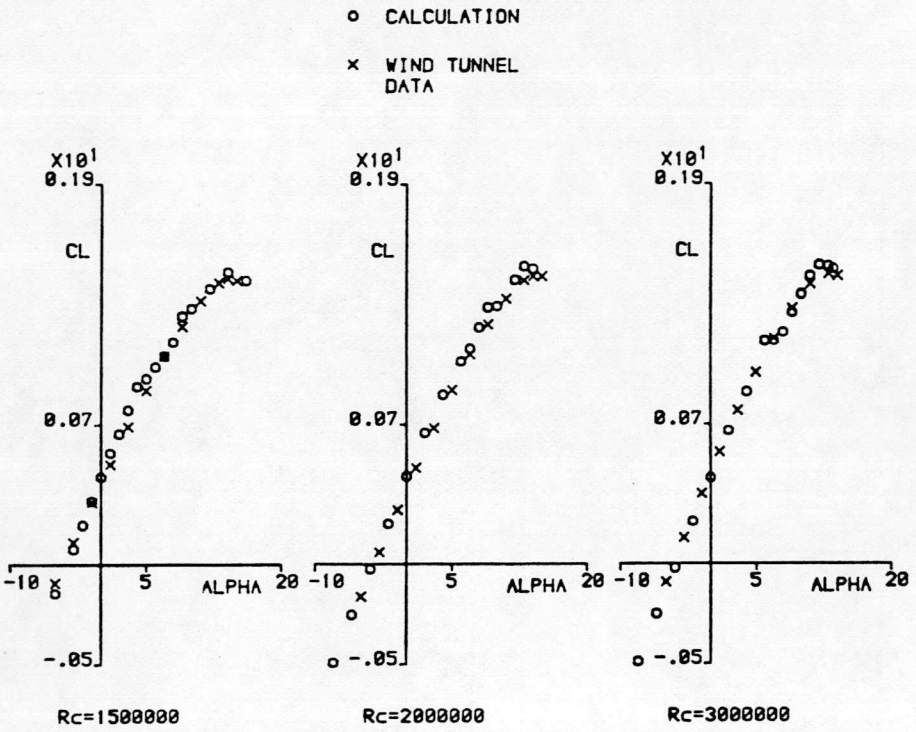

Fig. 10 Comparison of calculation with wind tunnel data for the NACA-4412 at three Reynolds numbers.

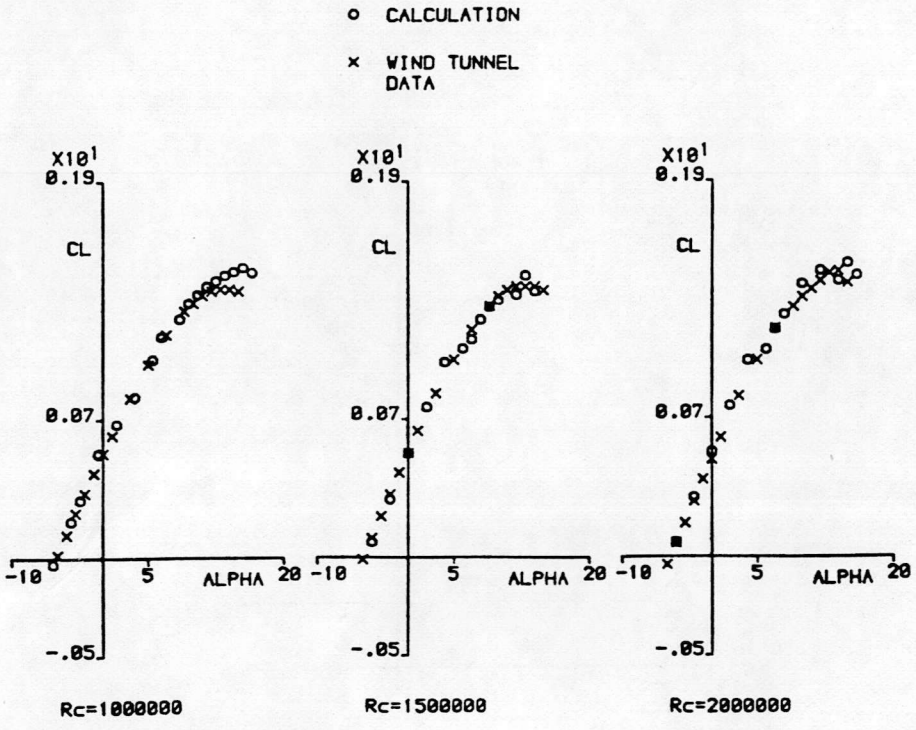

Fig. 11. Comparison of calculation with wind tunnel data for the NACA-4415 at three Reynolds numbers.

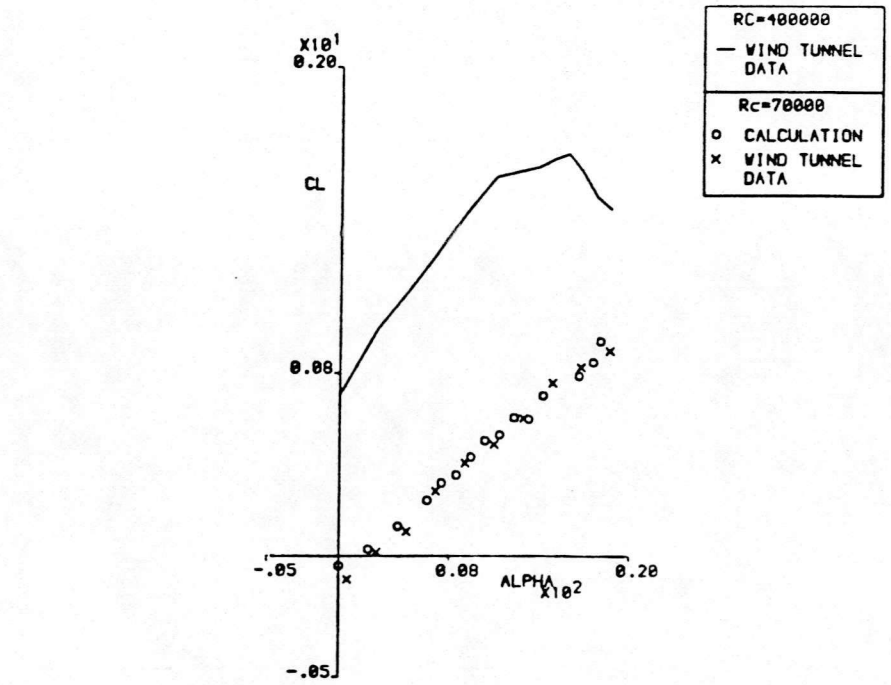

Fig. 12. Comparison of Cl at Rc=70000 with calculation and with that obtained at Rc=400000 for the GU25-5(11)8 aerofoil.

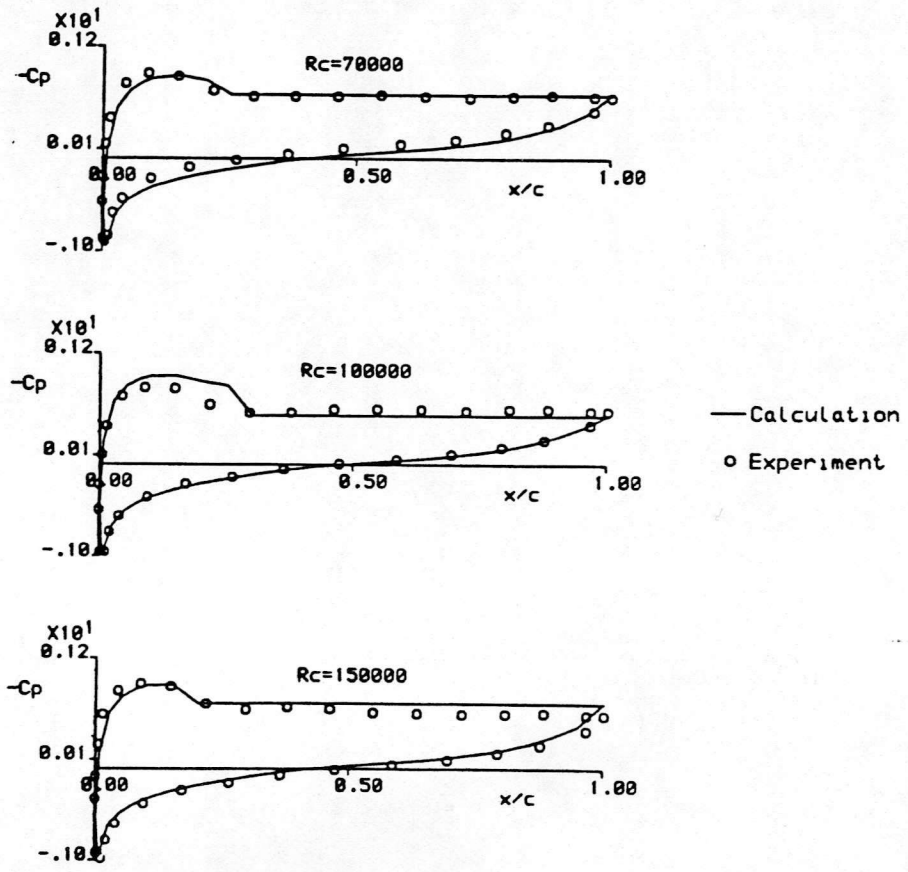

Fig. 13. Comparison of calculated and experimental Cp distributions for the GU25-5(11)8 aerofoil at 12.6 Degrees for three Reynolds numbers.